

# ON THE HIGH TEMPERATURE BENDING STRENGTH OF CASTABLES

#JIRÍ HAMÁČEK\*, JAN MACHÁČEK\*, JAROSLAV KUTZENDÖRFER\*,  
BOHUMIL KORSA\*\*, JAKUB FIALA\*\*

\*Department of Glass and Ceramics, Institute of Chemical Technology,  
Technická 5, CZ-16628 Prague, Czech Republic

\*\*Žárohmoty, Ltd., Keramická 214, CZ-330 11 Třemošná, Czech Republic

#E-mail: Jiri.Hamacek@vscht.cz

Submitted March 28, 2012; accepted June 19, 2012

**Keywords:** Hot modulus of rupture, Bending strength, Low cement refractory castables

*The hot moduli of rupture (HMOR) measurements have been performed for the low-cement castable (LCC), the ultra-low cement castable (ULCC), and the no-cement castable (NCC). All castables contained SiO<sub>2</sub>-Al<sub>2</sub>O<sub>3</sub> based aggregates (burned fireclay and kaolin). The experimental data points have been described using the model based on the Varshni approach within the temperature region 1000-1200°C and by the model based on the Adam-Gibbs theory above 1400°C. A smooth but distinct transition between both temperature regions has been observed. The limits and applicability of the models have been analyzed. At lower temperature the loss of strength of castables was attributed to weakening of bonds most probably in the frontal process zone of cracking. At higher temperature, the liquid phase causes slowing down of the crack propagation by formation of the viscous bridging in the following wake region. And finally, at very high temperatures, the castable behaves as very viscous suspension which can be described using models originally developed for molten glasses.*

## INTRODUCTION

The creep and mechanical properties of the refractory monoliths are important for their applicability at high temperature. The highest temperature of use strongly correlates with these properties. However, mechanical properties measured at room temperature after firing are of marginal importance for the behavior of refractories at working temperatures and they serve only for the rough appraisal of their quality [1, 2].

Among the high temperature properties, the refractoriness under load is conventionally measured [3]. Then, the creep behavior [4], i.e. the time dependence of creep at constant temperature. Recently, other important high temperature mechanical properties have been standardized [1]. In the first place, we should mention the hot modulus of rupture (HMOR) [5], and, alternatively, the high temperature compressive strength which might be tested as well.

The hot modulus of rupture provides the indication of a refractory material about its flexural strength at elevated temperatures. It is the true indicator of the suitability and performance of a refractory at high temperatures [6, 7].

As for refractory castables, aluminate cement (the Al<sub>2</sub>O<sub>3</sub>-CaO system) is mostly used as a binding component and granulated refractory materials from the Al<sub>2</sub>O<sub>3</sub>-SiO<sub>2</sub> system are used as aggregates [2, 8, 9]. According to the cement contents, the castables are

commonly subdivided into low cement castables (LCC), ultra-low cement castables (ULCC), and no-cement castables (NCC).

The aim of this work is to describe and discuss how the experimentally measured HMOR of LCC, ULCC, and NCC castables depends on temperature. For this purpose, we adopted two models having been derived ab initio for other physical phenomena but as we believe which are related to the problem addressed by our study.

## EXPERIMENTAL

The sample castables with various cement contents were prepared as LCC, ULCC, and NCC. Burned fireclay and burned kaolin were used as aggregates; aluminate cement and SiO<sub>2</sub> sol were used as binding agents in LCC (ULCC) and NCC, respectively. The list of components is given in Table 1. The chemical composition of the castables is seen in Table 2.

The rectangular testing pieces (3×3×15 cm) were heated up to 800°C by the rate of 100°C/h and fired for 2 hours. The samples of castables were only prefired to be used in modeling of behavior of real castables in operation. The samples fired at a single temperature higher than the chosen temperatures of measurements would behave as classical fired refractory materials.

Then, the hot modulus of rupture (HMOR) was measured in the temperature region from 1000°C to

1600°C by the three-point bending method. The heating rate was 5°C/min and the dwell time was 1 hour. Some examples of the ruptured testing pieces are shown in Figure 3.

Table 1. Components of the castables: (+) present and constant in all the castables, (>) present but decreasing in the line LCC, ULCC, and NCC, (<) increasing in the line LCC, ULCC, and NCC, and (-) absent.

Component	LCC	ULCC	NCC
aluminate cement (Gorkal 70)	>	>	-
SiO <sub>2</sub> sol (Tosil 40)	-	-	+
additives (deflocculants, retarders)	+	+	+
PP - fibers	+	+	+
reactive Al <sub>2</sub> O <sub>3</sub> (Martoxid)	<	<	<
micro-silica (RW-Fuller)	+	+	+
burned fireclay (Chamotte A111)	+	+	+
burned kaolin (Mulcoa 45)	+	+	+

Table 2. Chemical composition of the castables (wt.%). Minor components are not included.

	LCC		ULCC		NCC	
	matrix	total	matrix	total	matrix	total
Al <sub>2</sub> O <sub>3</sub>	71.3	52.7	74.1	53.3	65.3	51.6
SiO <sub>2</sub>	21.8	45.8	21.8	45.8	34.7	48.4
CaO	6.9	1.5	4.1	0.9	-	-

### THEORETICAL MODELS

Although the HMOR of castables generally depends on the microstructure, phase changes, chemical reactions, and other factors which somehow depend on temperature, the models proposed in this work leave them aside and focus on the energetics of atomic bonds and clusters. This approach can be justified by the fact that the high temperature processes are related to bond changes of the atomic structure.

#### The Varshni theory based model

Supposing a direct proportionality of the HMOR temperature dependence and the temperature dependence of elastic properties of solids (and neglecting possible phase transformations, chemical reactions, sintering, and the influence of microstructure), we may say that the strength of a solid body is given by the strength of bonds in it. This simple idea is implemented in the model developed by Varshni [10] which describes a downfall of elastic constant values with increasing temperature.

In this work, the Varshni theory (VT) based model is adopted for the temperature dependence of HMOR,  $\sigma$ , by the following equation:

$$\sigma = A - \frac{B}{\exp(C/T) - 1} \quad (1)$$

where  $T$  is thermodynamic temperature and  $A$ ,  $B$ , and  $C$  are parameters. The physical background of the original Varshni model is based on the direct proportionality of the elastic constant,  $c_{i,j}$ , and the mean energy per oscillator,  $\bar{\epsilon}$ , having been proposed by Liebfried and Ludwig [11]:

$$c_{ij} = c_0 (1 - D\bar{\epsilon}) \quad (2)$$

where  $c_0$  and  $D$  are parameters depending on the type of crystal or model.

Varshni substituted the mean energy per oscillator by the one calculated from the Einstein model of a solid:

$$\bar{\epsilon} = \frac{1}{2} h\nu + \frac{h\nu}{e^{h\nu/kT} + 1} \quad (3)$$

The Equation 1 emerges from Equation 2 and 3 by substitution and leaving the parameters free to be determined from experimental data. In this perspective, the parameter  $A$  introduces the maximal HMOR value, and the  $B$  and  $C$  parameters are proportional to a certain typical frequency of oscillations in a solid.

#### The Adam-Gibbs theory based model

Adam and Gibbs developed an Arrhenius-type expression [12] for the temperature dependence of viscosity where the activation energy for viscous flow was related to the configurational entropy of small structural units within the liquid. Since the size of these units changed with temperature so did the activation energy [13]. Supposing proportionality of HMOR and viscosity at high temperature at which solid particles are immersed in a viscous liquid we may write:

$$\ln \sigma = A' + \frac{B'}{T \ln(T/C')} \quad (4)$$

where  $T$  is the thermodynamic temperature,  $A'$  is the pre-exponential factor,  $B'$  is the activation barrier, and the  $\ln(T/C')$  term comes from the configurational entropy.

### RESULTS AND DISCUSSION

The experimental values of the HMOR of LCC, ULCC, and NCC testing pieces are collected in Table 3 and plotted in Figure 1 to emphasize the influence of a cement addition. It is seen that the increasing content of CaO in a castable causes an overall decrease in HMOR. On the other hand, the major features of the HMOR curves seem to be very similar, i.e. the maxima of HMOR at 1000°C, a steep fall between 1100°C and 1250°C, then a flat plateau approximately between 1300°C and

1400°C, followed by a gentle slope from 1400°C on. The lowest value of HMOR (0.8 MPa) is in the LCC system at 1500°C. The plateau is best pronounced in the NCC system.

The presence of the transition region indicates that the mechanism of rupture changes considerably with increasing temperature. It may be connected with formation of liquid phase preferentially in the matrix. This idea can be partly supported by the micrographs of thin sections of the LCC castable shown in Figure 4 where is seen that the transparency of the matrix is much higher in the sample exposed at 1500°C comparing with 1000°C and 1300°C. Moreover, the sample exposed at 1500°C contains the largest amount of micro-cracks. From the mineralogical point of view, the thin sections were

Table 3. Hot modulus of rupture (experimental data).

Temperature (°C)	HMOR [MPa]		
	LCC	ULCC	NCC
1000	12.4; 12.1	13.3	14.7
1100	11.8; 10.8	12.4	13.3
1150	8.9	11.1	10.4
1200	6.5; 6.4	7.0	6.9
1250	3.6	4.1	5.5
1300	2.2; 2.1	2.6	4.4
1400	1.6; 1.5	2.3	4.0
1450	–	1.8	3.0
1500	0.8; 0.9	1.4; 1.5	1.8; 1.9
1525	–	1.2	–
1550	–	0.9	1.3; 1.3
1600	–	1.3; 1.3	1.3; 1.1

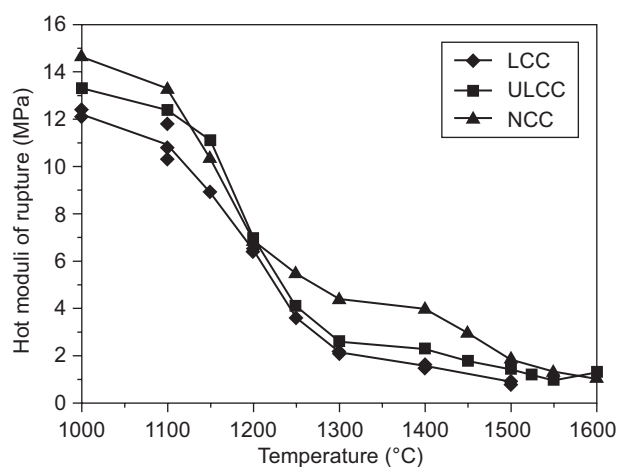


Figure 1. Comparison of the experimental HMOR of the LCC, ULCC, and NCC testing pieces. The lines serve only as guides to the eye.

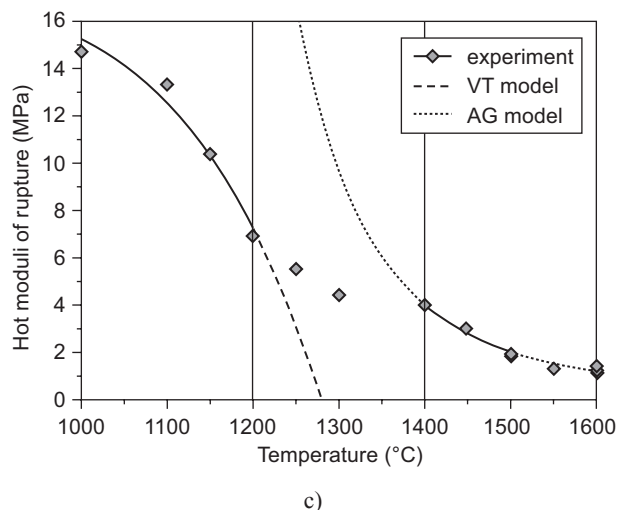
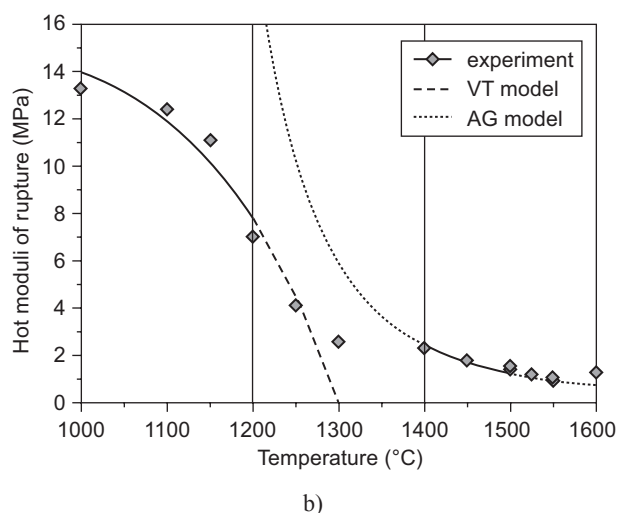
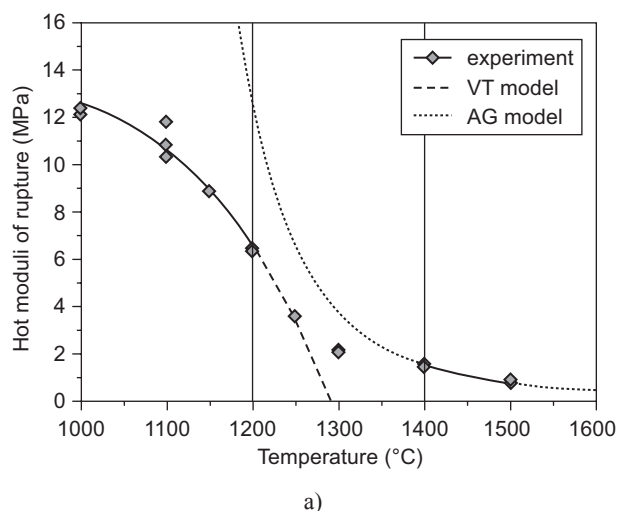


Figure 2. HMOR of the LCC (a), ULCC (b), and NCC (c) castables. The vertical lines delineate the transition region between the lower temperature region where the VT model has been applied and the high temperature region where the AG model has been used. The dashed lines extrapolate the models into the transition region and to higher temperature.

found practically identical. They consist of fine-grained aggregates containing mostly mullite; SiO<sub>2</sub> phases; and amorphous matrix. Other crystalline phases containing calcium, e.g. anorthite or gehlenite were not identified.

For the regression analysis of HMOR as a function of temperature, two regions were chosen: the first region between 1000-1200°C, where is located the steepest fall of HMOR; and the third region between 1400-1500°C, where the HMOR curve is flat. The second (transition)

region in between was not used for fitting. The VT model (Equation 1) was applied in case of the first region and its parameters are collected in Tab. 4. The parameters of the AG model (Equation 4) applied in the third region are in Table 5. The curves of both models and the experimental data-points are shown in Figure 2. The curves are extrapolated into the transition region between 1200°C and 1400°C. Moreover, the curves of the AG model are extrapolated up to 1600 °C to predict HMOR at very high temperatures (Figure 2, and the last two rows in Table 5). This can be done under the conditions of finding the threshold between the second transition region and the third region in which at least three data points must be known.

It should be emphasized that the *B'* and *C'* parameters of the AG model were forced to be the same in all three systems during the least-squares fitting. It indicates that the parameter *A'* (i.e. the pre-exponential factor) is the most important in exploring the role of the CaO addition. Similarly, by fixing the *B* and *C* in the VT model, it might be shown that the parameter *A* (i.e. the maximum HMOR) is most important in exploring the role of CaO addition.

Two models were needed to cover most of the experimental data. At lower temperature the loss of strength of castables was attributed to weakening of bonds most probably in the frontal process zone of cracking (Figure 5). At higher temperature, the liquid phase causes slowing down of the crack propagation by formation of the viscous bridging in the „following wake region“ [14]. And finally, at very high temperatures, the castable behaves as very viscous suspension which can be described using models originally developed for molten glasses.

Table 4. The parameters of the VT model fitted between 1000-1200 °C. The  $T_{0MPa}$  value is the predicted temperature at which a HMOR value should reach zero.

VT model	LCC	ULCC	NCC
<i>A</i> (MPa)	13.9	15.3	17.0
<i>B</i> (MPa)	466385	495736	470711
<i>C</i> (K)	16309	16343	15880
$T_{0MPa}$ (°C)	1292	1300	1279

Table 5. The parameters of the AG model fitted between 1400 and 1500 °C. The *B'* and *B'* parameters were forced to be the same in all three systems. The values  $\sigma_{1550°C}$  and  $\sigma_{1600°C}$  are the HMOR predictions at 1550°C and 1600°C.

AG model	LCC	ULCC	NCC
<i>A'</i> (MPa)	0.009	0.015	0.024
<i>B'</i> (MPa.K)	5724	= 5724	= 5724
<i>C'</i> (K)	858	= 858	= 858
$\sigma_{1550°C}$ (MPa)	0.6	0.9	1.5
$\sigma_{1600°C}$ (MPa)	0.5	0.7	1.2

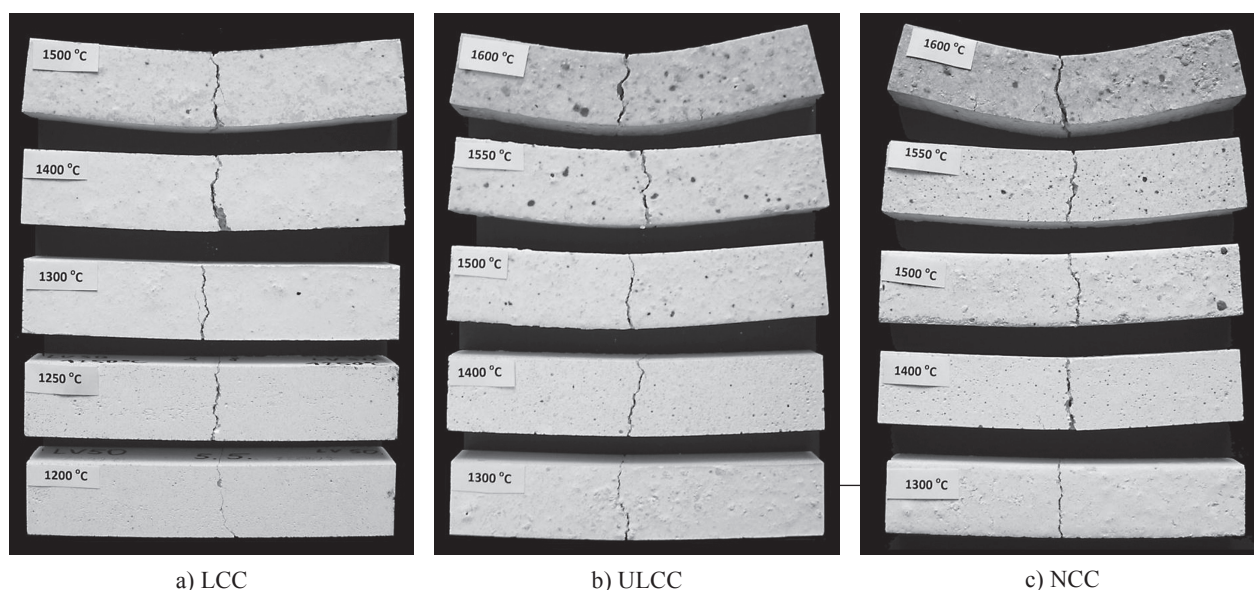
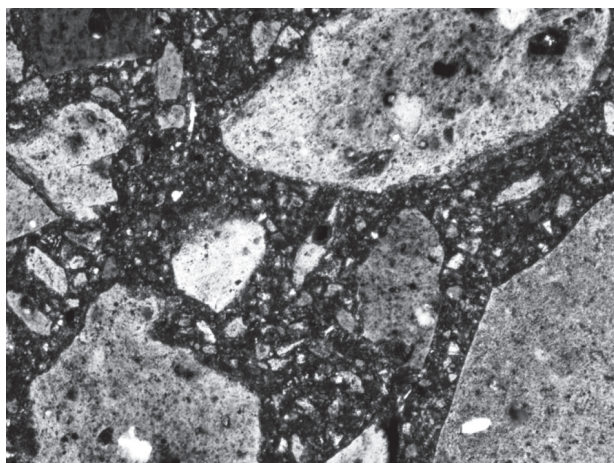
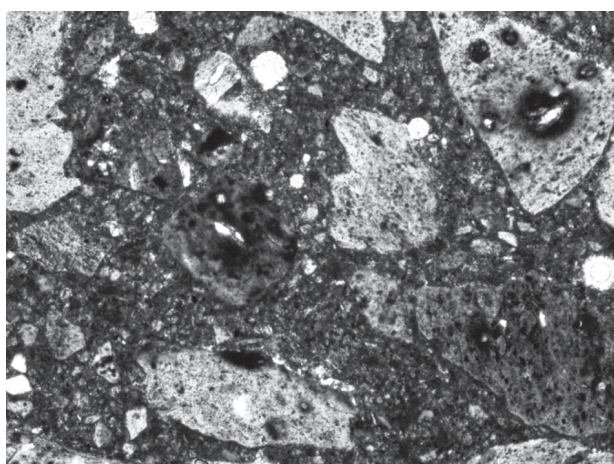


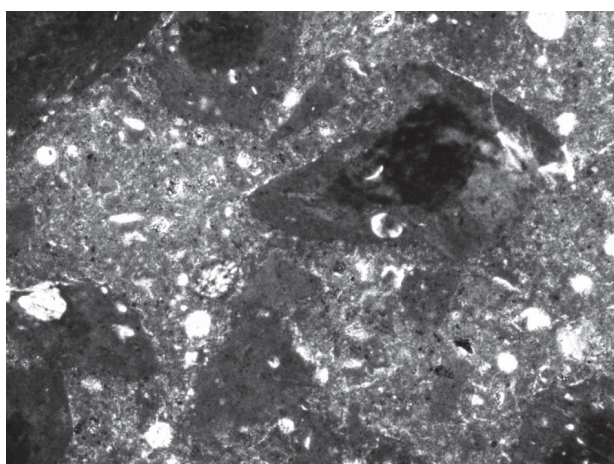
Figure 3. Ruptured samples of the LCC (a), ULCC (b), and NCC (c) castables (exposure temperature is shown for each sample).



a) 1000°C



b) 1300°C



c) 1500°C

Figure 4. Thin sections of the LCC castable ruptured at 1000°C (a), 1300°C (b), and 1500°C (c).

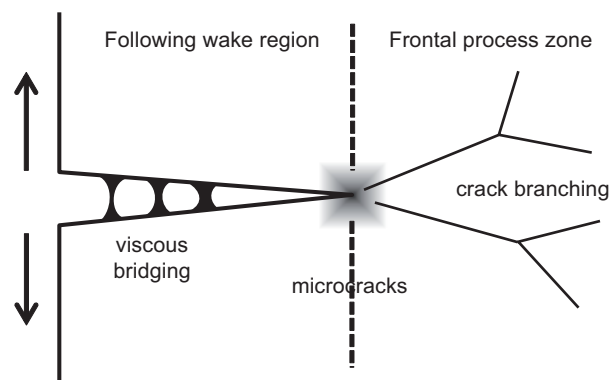


Figure 5. Cracking of castables. Freely according to [14].

## CONCLUSIONS

The hot moduli of rupture measurements have been performed for the low-cement castables, ultra-low cement castables, and no-cement castables. All castables contained  $\text{SiO}_2\text{-Al}_2\text{O}_3$  based aggregates (burned fireclay and kaolin). The experimental data points have been described using the model based on the Varshni approach within the temperature region 1000-1200°C and by the model based on the Adam-Gibbs theory above 1400°C. A smooth but distinct transition between both temperature regions has been observed. The limits and applicability of the models have been analyzed. At lower temperature the loss of strength of castables was attributed to weakening of bonds most probably in the frontal process zone of cracking. At higher temperature, the liquid phase causes slowing down of the crack propagation by formation of the viscous bridging in the “following wake region”. And finally, at very high temperatures, the castable behaves as a very viscous suspension which can be described using models originally developed for molten glasses.

## Acknowledgements

This work was supported by the Grant Agency of the Czech Republic through the grant No. P108/10/1631. This study was also a part of the project No 2A-1TP1/063, “New glass and ceramic materials and advanced concepts of their preparation and manufacturing”, realized under financial support of the Ministry of industry and trade.

## References

1. Kutzendörfer J., Tomšů F.: *Žárovzborné materiály I*, Silikátová společnost ČR, Praha 2008. (in Czech)
2. Tomšů F., Palčo Š.: *Žárovzborné materiály IV*, Silikátová společnost ČR, Praha 2009.
3. ČSN EN 993-8, “*Refractoriness under load*”.

4. ČSN EN 993-9, "Creep in compression".
  5. ČSN EN 993-7, "Modulus of rupture at elevated temperature".
  6. Banerjee S. in: *Refractories Handbook*, p. 1-10, Ed. Schacht C.A., Marcel Dekker Inc., New York 2004.
  7. Hamacek J., Machacek J., Kutzendorfer J., Korsá B., Fiala J. in: Proc. 17th International Conference on Refractories, p. 295-300, Ed. Czech Silicate Society, Prague 2011.
  8. Altun I.A.: *Cement Concrete Res.* 31, 1233 (2001).
  9. Krebs R. in: *Refractories Handbook*, p. 287-333, Ed. Schacht C.A., Marcel Dekker Inc., New York 2004.
  10. Varshni Y.: *Physical Review B* 2, 3952 (1970).
  11. Liebfried G., Ludwig W.: *Solid State Phys.* 12, 275 (1961).
  12. Adam G., Gibbs J.H.: *J. Chem. Phys.* 43, 139 (1965).
  13. Varshneya A.K.: *Fundamentals of inorganic glasses*, p. 189, Academic Press, London 1994.
  14. Bradt R.C., Harmuth H.: *Refractories Worldforum* 3, 129 (2011).
-